Simultaneous Dual-frequency Range Conductivity Mapping MR Method for Tissue Characterization: In Vivo Canine Brain Disease Model Study

Woo Chul Jeong[1], Min Oh Kim[2], Saurav ZK Sajib[1], Ji Eun Kim[1], Hyung Joong Kim[1], Oh In Kwon[3], Dong Hyun Kim[2], and Eung Je Woo[1]
[1]Kyung Hee University, Yongin, Gyeonggi, Korea, [2]Yonsei University, Seoul, Korea, [3]Konkuk University, Seoul, Korea

Target audience

This study might be helpful to the researchers who are interested in MR-based electrical tissue property mapping such as MREIT and MREPT.

Purpose

The purpose of this study is to show the potentials of simultaneous dual-frequency range conductivity mapping MR method providing frequency-dependent tissue contrast through *in vivo* canine brain abscess and ischemia model imaging experiments.

Methods

Ten healthy beagles (5 for abscess and 5 for ischemia) were used. Brain abscess was induced by a direct inoculation method (*Staphylococcus pseudintermedius*). We induced a regional ischemia by occluding the left middle cerebral artery. For imaging experiment, we anesthetized the dog with intramuscular injection of 0.2 ml/kg Tiletamine and Zolazepam. Twenty minutes later, we clipped hair at four locations on the head where we attached four electrodes. Inside the shield room, we kept the anesthesia using a veterinary anesthesia machine system. The experimental protocol was approved by IACUC. Imaging objects were positioned inside the bore of a 3 T MRI scanner. Using a constant current source, we injected currents in two mutually orthogonal directions between two pairs of electrodes facing each other. The injection current amplitude was 5 mA with the total pulse width of 30 msec. The multi-spin echo ICNE pulse sequence was used for imaging experiments.[1] Image parameters were TR/TE = 800/15, 30, 45, 60 (4 echoes) msec, FOV = 180 × 180 mm^2, slice thickness = 4 mm, number of averages = 8, matrix size = 128 × 128, number of slices = 8 and total scan time = 30 min. After imaging experiment, magnetic flux density induced by externally injected currents and B_1^+ phase map generated by removing the effects of injected currents were determined from the same data set for low- and high-frequency conductivity images.[2]

Results and Discussion

Figure 1 shows dual-frequency conductivity images of brain abscess. Figure 1a-c was obtained at 12 hours after the induction. The central area (black arrow) represents a mixture of necrosis and inflammatory cells. The surrounding area (white arrow) consists of hemorrhage, inflammatory cells and peripheral edema. The low- and high-frequency conductivity (Fig. 1b and c) show higher contrast in the central area due to the highly conductive tissue conditions. The surrounding area shows similar conductivity compared with the opposite normal gray matter. Figure 1d-f was obtained at 20 hours. The low-frequency conductivity image shows decreased contrast in the central areas (Fig. 1e) due to the ring-shape membrane and hemorrhage. The increased conductivity at high-frequency (Fig. 1f) reveals that the high-frequency current can penetrate through the region regardless of the ring-shape membrane. In the surrounding area, the high-frequency conductivity image shows increased contrast than low-frequency due to the residual peripheral edema with highly conductive cell state.

Figure 2 shows *in vivo* low- and high-frequency conductivity images of regional ischemia. The low-frequency conductivity image (Fig. 2b) shows decreased values due to the cell swelling while high-frequency (Fig. 2c) shows similar values compared with the opposite normal gray matter. Since the cell membrane behaves as an electrical insulator, the injected current at low frequency could not penetrate the cell membrane. For this reason, their apparent conductivity was lower than its surroundings. In contrast, the high-frequency conductivity image shows its values without being affected by the cell membrane.

Table 1 summarizes the measured low- and high-frequency conductivity values from both the brain abscess and ischemia model. C1 to C3 represents the first, second and third canine brain sample. The conductivity values of central and surrounding areas in abscess lesions are marked ROI (region-of-interest) A and B. ROI C and D represent ischemic lesion and contralateral normal area, respectively.

Conclusion

In this study, we evaluated the MR-based electrical tissue property mapping at dual-frequency and highlighted their distinct features from *in vivo* disease model animal imaging experiments.

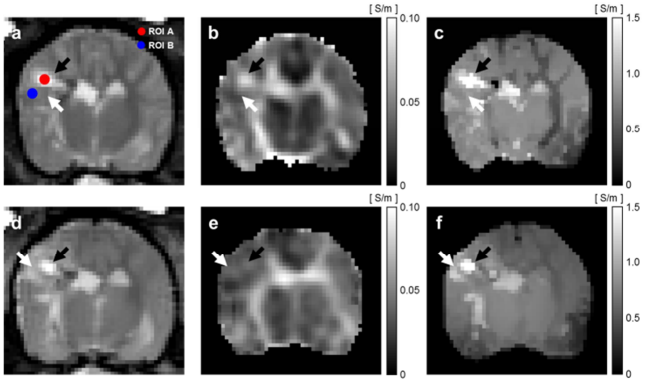

Fig. 1. Simultaneous dual-frequency range conductivity images of *in vivo* canine brain abscess obtained at 12 (a-c) and 20 (d-f) hours after the induction.

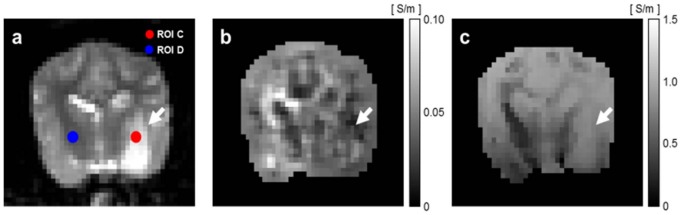

Fig. 2. *In vivo* low- and high-frequency conductivity images of ischemic canine brain. (a) is MR magnitude, (b) and (c) are low- and high-frequency conductivity images.

Table 1. Measured conductivity values of *in vivo* brain disease models. Absolute values (mean ± SD) of low- and high-frequency conductivity were calculated with a ROI size of 5×5 pixels shown in Figs 1a and 2a.

Conductivity [S/m] / Frequency		Abscess				Ischemia	
		At 12 hours		At 20 hours			
		ROI A	ROI B	ROI A	ROI B	ROI C	ROI D
Low	C1	0.101 ± 0.025	0.065 ± 0.021	0.059 ± 0.012	0.069 ± 0.016	0.049 ± 0.011	0.093 ± 0.022
	C2	0.115 ± 0.011	0.078 ± 0.016	0.069 ± 0.014	0.074 ± 0.017	0.058 ± 0.013	0.080 ± 0.017
	C3	0.097 ± 0.023	0.072 ± 0.018	0.078 ± 0.019	0.069 ± 0.021	0.065 ± 0.018	0.092 ± 0.023
High	C1	0.968 ± 0.156	0.683 ± 0.216	1.009 ± 0.194	0.689 ± 0.233	0.683 ± 0.217	0.453 ± 0.133
	C2	1.259 ± 0.216	0.739 ± 0.258	1.303 ± 0.217	0.722 ± 0.203	0.625 ± 0.199	0.389 ± 0.116
	C3	1.023 ± 0.116	0.722 ± 0.219	1.102 ± 0.253	0.731 ± 0.324	0.559 ± 0.154	0.473 ± 0.112

References

1. Minhas AS, Jeong WC et al. Experimental performance evaluation of multi-echo ICNE pulse sequence in magnetic resonance electrical impedance tomography. Magn. Reson. Med. 2011;66:957-965.
2. Kim HJ, Jeong WC et al. Simultaneous imaging of dual-frequency electrical conductivity using a combination of MREIT and MREPT. Magn. Reson. Med. 2014;71:200-208.